

Imaging of pathology involving the space around the hepatic veins: "perivenous pattern"

Ali Devrim Karaosmanoğlu 

Mehmet Ruhi Onur 

Mustafa Nasuh Özmen 

Deniz Akata 

Muşturay Karçaaltıncaba 

ABSTRACT

We aimed to illustrate diseases involving the potential space around the hepatic veins. Perivenous halo sign can be seen in patients with congestive heart failure or fluid overload. Perivenous involvement can be observed in patients with alcoholic fatty liver disease, which can be focal or diffuse. Metastasis and primary liver tumor spread can also involve this space most likely due to involvement of lymphatics around hepatic veins.

The liver may be affected by various benign and malignant disorders. The mode of spread to the liver parenchyma may include hematogenous or lymphatic routes as well as direct extension from neighboring anatomic structures. In this article, by using the term "perivenous space" we refer to the parenchymal areas surrounding the hepatic veins. Hepatic veins received little attention compared with portal veins in imaging literature (1). In the same manner, the perivenous space also gained minimal to no attention from the imaging community. Compared with several articles studying the role of imaging in the evaluation of the periportal space, not much has been written about the perivenous space. Perivenous halo sign occurs due to accumulation of fluid in perivenous space resulting from congestion in the setting of congestive heart failure or fluid overload. Fat deposition, inflammatory infiltration, and neoplastic infiltration may be seen in the perivenous space around the liver. In this article, we first describe the imaging anatomy of this space and, subsequently, the non-neoplastic and neoplastic processes involving this anatomic compartment.

Anatomy

Hepatic veins represent the main venous outflow tract of the liver parenchyma. Despite the dual vascular supply nourishing the liver parenchyma, the outflow is almost solely via the hepatic veins. They also play a major role in the anatomic segmentation of the liver, defined by French surgeon Claude Couinaud (2). Based on Couinaud's definition, the liver is divided into eight segments with portal vein branches at the center and hepatic veins at the periphery.

In a normal liver there are 3 hepatic veins; namely, right, middle, and left hepatic veins. These hepatic veins drain into the retrohepatic portion of the inferior vena cava (IVC), approximately 2 cm caudal to the right atrium. The right hepatic vein generally joins the IVC as a separate trunk, while in 65%–85% of the patients middle and left hepatic veins form and share a common trunk before draining into IVC (3). There are several accessory hepatic vein branches described but we will not discuss them in detail for the sake of brevity of this article. Interested readers may refer to several excellent articles published in the literature regarding this topic (3–6).

Hepatic lymphatic vessels deserve attention in understanding the perivenous pattern. The hepatic lymphatic system is mainly divided into superficial and deep networks (7). The deep hepatic lymphatic system mainly surrounds the portal vein branches and is responsible for 80% of the lymphatic drainage of the liver (8). Along the portal tracts these lymphatic vessels converge into larger vessels (around 12–15 vessels) which eventually drain

Department of Radiology (M.K. ✉ musturayk@yahoo.com), Liver Imaging Team, Hacettepe University School of Medicine, Ankara, Turkey.

Received 21 December 2017; revision requested 11 January 2018; last revision received 27 January 2018; accepted 29 January 2018.

DOI 10.5152/dir.2018.17510

You may cite this article as: Karaosmanoğlu AD, Onur MR, Özmen M, Akata D, Karçaaltıncaba M. Imaging of pathology involving the space around the hepatic veins: "perivenous pattern". *Diagn Interv Radiol* 2018; 24:77–82.

into the hepatic hilar lymph nodes. These hepatic lymph nodes are mainly located in the lesser omentum and they eventually drain into cisterna chyli, which represents the dilated origin of the thoracic duct which is the largest lymphatic vessel of the body. As mentioned above, despite the fact that the periportal compartment is where the main deep lymphatic network is located, a not insignificant portion of the deep drainage is via the perivenous lymphatic vessels which mainly reside around the hepatic veins. The perivenous lymphatic vessels finally converge into 5–6 large vessels which eventually drain into posterior mediastinal lymph nodes (7).

The superficial hepatic lymphatic system is a part of the liver surface (7). These superficial vessels originate from the convex and inferior surfaces of the liver and finally drain into several different lymph nodes.

Non-neoplastic perivenous pathologies

Lymphedema

By definition, lymphedema refers to the abnormal distension of the lymphatic vessels. The underlying etiology may be either related to overproduction of the lymphatic fluid or to the blockade of distal lymphatic flow. Lymphedema is mostly detected in the periportal space; however, perivenous lymphedema is not uncommon. Several intra and extrahepatic disorders may promote lymphedema, including, but not limited to, hepatic inflammation, trauma, overhydration, pancreatitis, pneumonia, or pyelonephritis (7). Iatrogenic causes, mainly due to extensive surgical dissection in tumor surgery as well as liver transplantation, may also represent the underlying etiology in some patients (9).

Congestive hepatopathy, which basically refers to passive hepatic congestion in congestive heart failure, is an important and relatively common cause of perivenous lymph-

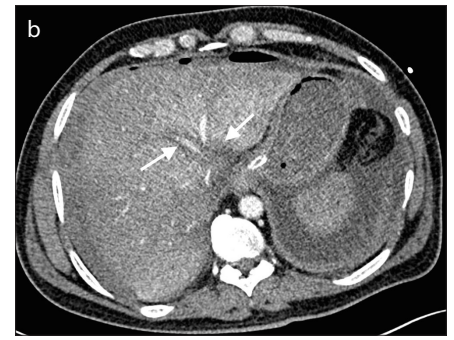


Figure 1. a, b. Panel (a) shows axial contrast-enhanced CT image of a 70-year-old female with known severe congestive heart failure and right upper quadrant discomfort. Linear hypoattenuating areas (arrows) are seen around the hepatic veins suggestive of mild perivenous lymphatic edema due to severe right heart failure. Panel (b) shows axial contrast-enhanced CT image of a 46-year-old male with known congestive heart failure referred for evaluation of presumptive ascites on physical exam. Marked perivenous edema (arrows) is seen around the hepatic veins.

edema. Increased hydrostatic pressure within the IVC and hepatic vein lumens subsequently gives rise to sluggish flow within the intrahepatic venous outflow network, which eventually may lead to nutmeg liver appearance and hepatocyte necrosis (10).

On imaging, perivenous lymphedema appears as a hypodense halo around the hepatic veins. On computed tomography (CT) studies, the engorged lymphatic vessels give rise to perivenous linear hypoattenuation, which might be reminiscent of conventional periportal halo (Fig. 1). Magnetic resonance imaging (MRI) may also be used in the evaluation of perivenous lymphedema and T2-weighted images can be especially helpful by clearly delineating the perivenous hyperintensity.

Perivenous fat deposition

Focal parenchymal fat deposition/sparing may mimic focal parenchymal liver lesions and definitive diagnosis may be difficult in some cases. Several imaging findings might be helpful for diagnosis of fatty pseudolesions over the true neoplastic/inflammatory masses. Among these findings, absence of mass effect in adjacent vascular/biliary structures, characteristic location, ill-defined lesion borders rather than round or oval shape (which are characteristic for true neoplastic lesions), contrast enhancement pattern similar to background liver parenchyma should be counted (11).

Perivascular fat deposition was first described by Hamer et al. in 2005 (12). The typical cross-sectional imaging finding of perivascular fatty infiltration is the tram-like configuration for vessel segments parallel to the imaging plane, and a ringlike or round configuration for vessel segments

perpendicular to the imaging plane (12) (Fig. 2). Perivenous fatty infiltration is generally bilobar (12). The absence of mass effect is one of the key imaging features for focal fat deposition within the liver parenchyma. Sonographic findings are generally nonspecific and the detection of perivascular involvement may be hard to perceive. CT and MRI are generally utilized as the problem-solving modalities in these patients. Signal loss on opposed phase images compared to in-phase images are diagnostic for perivenous fat deposition on MRI (Fig. 3).

Sinusoidal obstruction syndrome

Sinusoidal obstruction syndrome (SOS), also called as veno-occlusive disease, is thought to be related to chemotherapy- or radiation-induced destruction of hepatic microvasculature during cytoreductive treatment (13). Histologically, obliteration of the small hepatic venules with associated surrounding fibrosis and obstructed sinusoids from debris of necrotic endothelial cells are characteristic findings (14, 15). SOS is a relatively common adverse effect of chemotherapy regimens and stem cell transplantation. The reported incidence of SOS in patients treated for colorectal cancer with systemic chemotherapy was reported to be between 42% and 51%. Oxaliplatin use is a well-known risk factor for SOS development with a reported incidence of 51%–79%, compared with 21%–30% with chemotherapy regimens not including oxaliplatin (16–18).

In most of the cases, SOS does not cause any detectable symptoms per se; however, its detection is important in patients undergoing evaluation for liver resection to prevent potentially mortal liver failure es-

Main points

- Perivenous space refers to the adjacent structures surrounding the hepatic veins.
- Accumulation of fluid in the perivenous space, resulting from congestion in the setting of congestive heart failure or fluid overload, presents as the perivenous halo sign.
- Fat deposition, inflammatory infiltration, and neoplastic infiltration may be seen in the perivenous space around the liver.

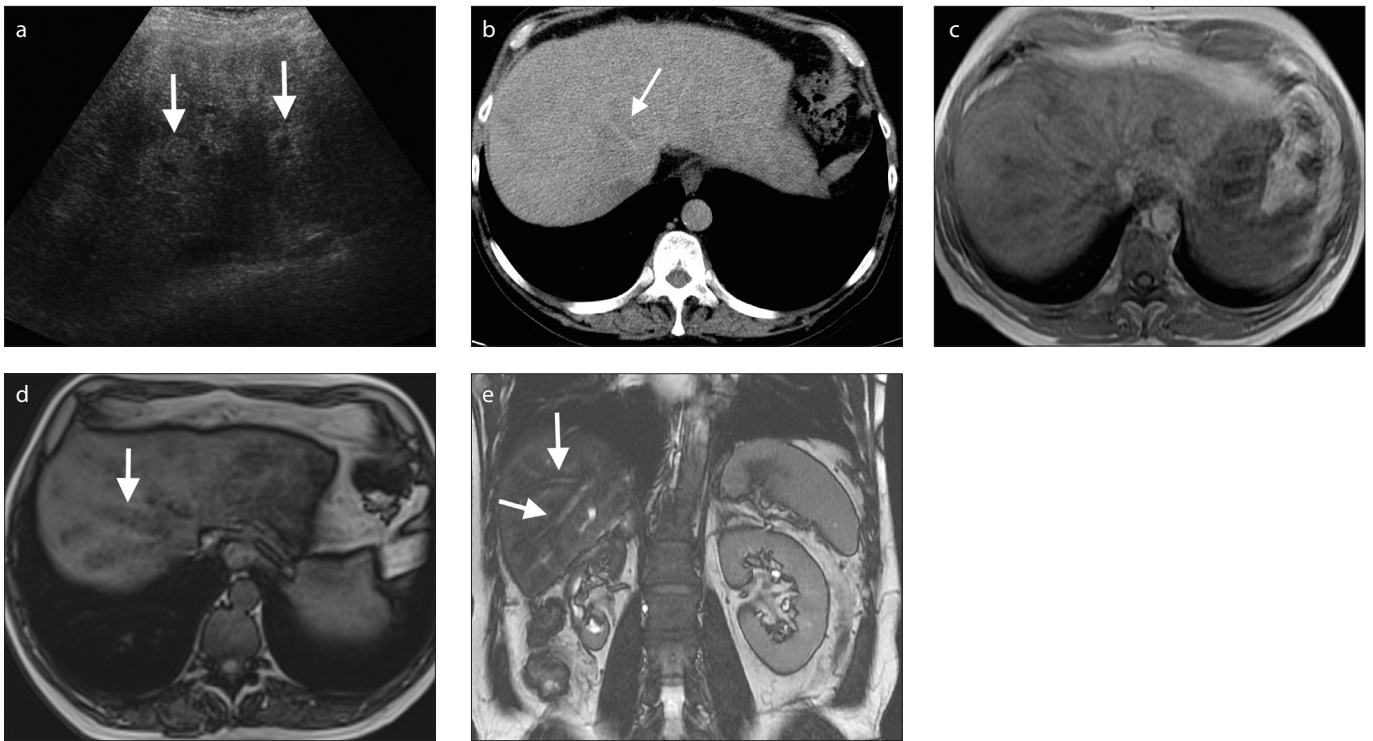


Figure 2. a–e. A 51-year-old male with chronic steroid use was referred for evaluation of the elevated serum liver enzymes. Gray-scale US image (a) reveals increased echogenicity (arrows) around the middle hepatic vein, with no evidence of mass effect on the vessel lumen. Axial contrast-enhanced CT image (b) of the same patient shows hypoattenuating areas around the middle hepatic vein corresponding to hyperechoic areas detected in the US exam. Axial in-phase dual echo magnetic resonance image (c) reveals no abnormal signal change in the liver parenchyma. Axial out-phase dual-echo image (d) demonstrates signal loss around the hepatic veins (arrows) with fat around the middle hepatic vein. Coronal true fast imaging with steady state precession (TRUE-FISP) image (TE: 2.3 ms) (e) demonstrates perivascular low signal intensity (arrows) representing perivascular fat.

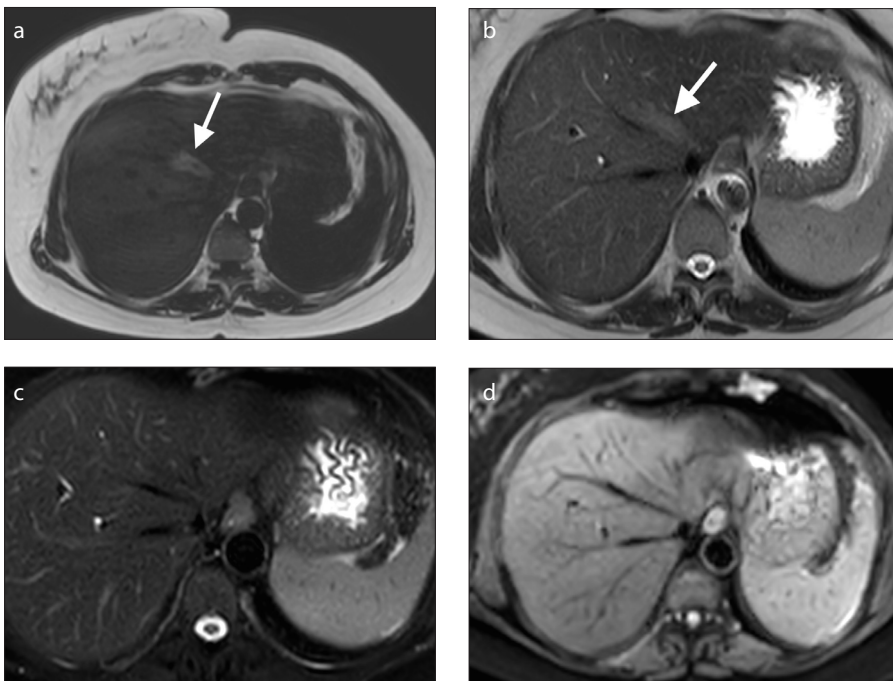


Figure 3. a–d. A 49-year-old female with known colon cancer who was referred for an abdominal CT scan for restaging purposes. Previous sonographic exam at an outside center revealed hyperechogenicity around the hepatic veins (images were not available for review). Axial T1-weighted (a) and T2-weighted (b) images reveal focal increased signal intensity (arrows) in the hepatic parenchyma surrounding the middle hepatic vein. Axial fat-suppressed T2-weighted image (c) reveals signal loss in the corresponding hyperintense areas detected on the T1- and T2-weighted images, confirming perivascular fat deposition. Diffusion-weighted image (d) demonstrates no restriction in this area.

pecially after surgery (19). Thus, the identification of SOS may be critical for optimum timing of surgery and also for the planning of further chemotherapy (20).

The typical imaging findings may not be present in all affected patients. The imaging findings are generally nonspecific; however, periportal edema, ascites, gallbladder wall thickening, heterogeneous parenchymal enhancement and hepatomegaly are suggestive imaging features when detected. Sonographic imaging findings are nonspecific, but reversal of flow in portal veins may be detected in some patients (21, 22). The presence of narrowed right hepatic vein caliber is also a reported CT finding (23).

MRI studies with the use of gadoxetic acid disodium (Gd-EOB-DTPA, Primovist or Eovist, Bayer Schering Pharma AG) appears to be a more sensitive method for detecting SOS and provided invaluable functional clues in a noninvasive manner. Gd-EOB-DTPA is a relatively new hepatocyte specific contrast agent which has recently gained wide popularity in liver imaging. Hepatobiliary phase images are generally acquired 20 minutes after contrast injection and this phase appears to be the most valuable part of the dynamic MRI of the liver. Reticular

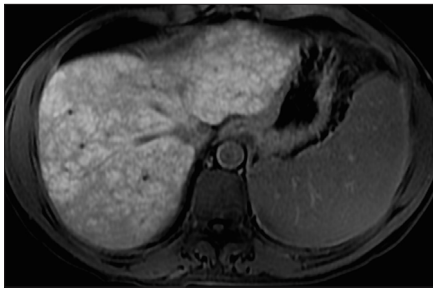


Figure 4. A 51-year-old woman with a history of colon cancer and elevated serum liver enzymes who underwent several treatment cycles of oxaliplatin-based chemotherapy regimens. Axial T1-weighted image in the hepatobiliary phase reveals areas of hypofunctioning liver parenchyma around the hepatic veins, which were attributed to SOS.

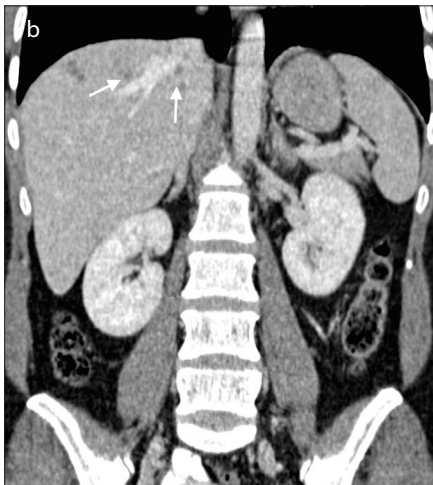
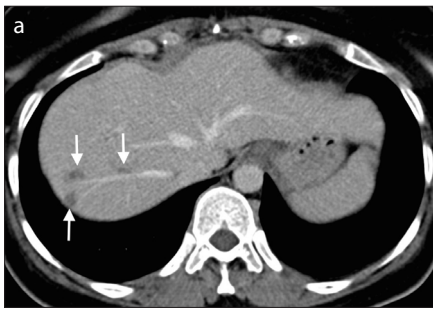


Figure 5. a, b. A 45-year-old male with newly onset fatigue and mildly elevated serum markers of inflammation. Axial (a) and coronal (b) contrast-enhanced CT images demonstrate small-sized low attenuating focal hypodense lesions (arrows) which later proved to be (by percutaneous aspiration) microabscesses caused by *Fasciola hepatica*. Abscesses are mostly located in the subcapsular areas as well as along the parenchyma neighboring the right hepatic vein.

type hepatic parenchymal hypointensity in this phase, in patients who underwent chemotherapy for liver metastases, appears to be a sensitive imaging finding for SOS (19) (Fig. 4). Graft-versus-host disease

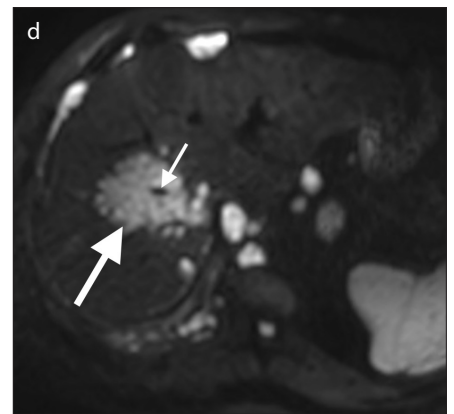
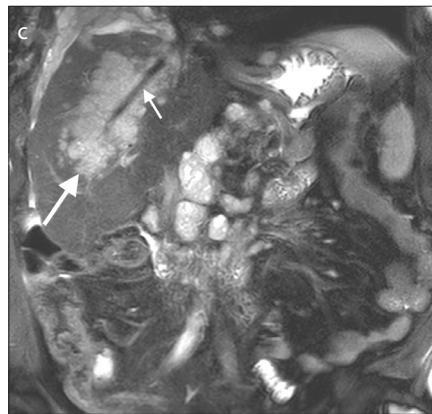
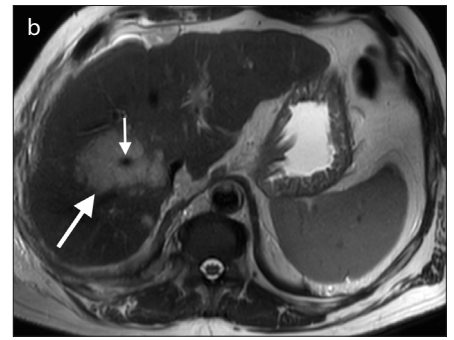
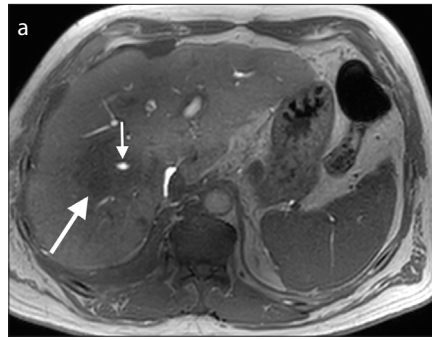


Figure 6. a–d. A 56-year-old male with known advanced stage lung cancer was referred for restaging. Axial T1-weighted contrast-enhanced image (a) demonstrates a hypointense ill-defined mass (long arrow) around the middle hepatic vein (short arrow). Axial (b) and coronal (c) T2-weighted images reveal the same mass as ill-defined hyperintense lesions (long arrows) around the middle hepatic vein (arrow). On diffusion-weighted image (d), lesions show severe diffusion restriction as areas of increased signal intensity. Subsequent percutaneous biopsy confirmed the metastasis.

(GVHD) may also develop in patients with a history of stem cell transplant and can manifest with symptoms similar to those of veno-occlusive disease and histopathologic evaluation may be necessary to confirm the diagnosis (23). The association of small bowel wall thickening in addition to other findings detected in SOS is more suggestive of GVHD than SOS (23).

Parasitic infection

Fascioliasis of the liver is caused by the trematode *Fasciola hepatica*. The life cycle of *Fasciola hepatica* in humans starts with ingestion of the parasite. The parasites then penetrate the duodenal wall and gain access into the peritoneal cavity with subsequent penetration into the liver parenchyma through the hepatic capsule. The spreading pattern of fascioliasis in the liver parenchyma is centripetal due to random migration of the parasites within the liver parenchyma. Intrahepatic bile ducts may be also be infiltrated which subsequently gives rise proximal bile duct dilatation (24). Imaging features of liver fascioliasis include

parenchymal heterogeneity, focal irregularly distributed small parenchymal abscesses with dilatation of the bile ducts. Endoluminal filling defects within the biliary system, ductal wall enhancement and periportal located enlarged lymph nodes may also be detected (25). Tract-like lesions might be encountered in the liver parenchyma, secondary to intraparenchymal migration of the parasites. Perivenous areas may also be affected in the course of the disease (Fig. 5).

Neoplastic perivenous pathologies

Metastases

Liver is one of the most commonly involved organs in patients with metastatic disease. Colon, breast, lung, and stomach should be counted among the most common primary tumors (26). Secondary neoplastic involvement of the liver far exceeds the incidence of primary hepatic tumors and hematologic seeding is the most common gateway to the liver parenchyma. Accurate and prompt detection of liver metastases is of critical importance for successful

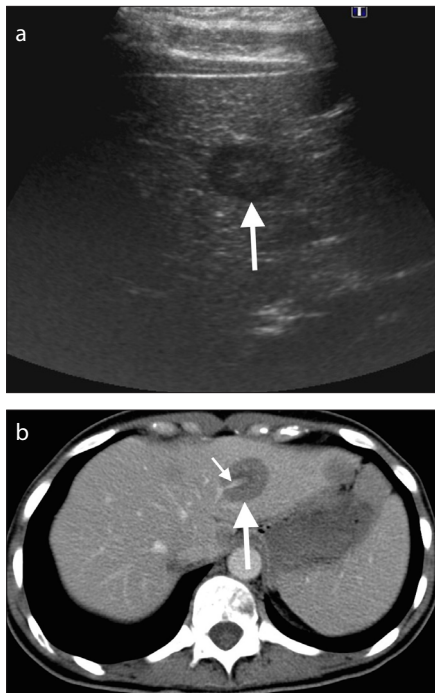


Figure 7. a, b. A 25-year-old female diagnosed lymphoma was referred for primary staging. Gray-scale US (a) reveals a hypoechoic solid mass (arrow) in the liver parenchyma. Axial plane contrast-enhanced CT image (b) confirmed the presence of the mass (long arrow). Also note the left hepatic vein traversing through the lesion (short arrow) with no evidence of luminal narrowing or obstruction. Subsequent percutaneous biopsy confirmed the lymphomatous deposition within the liver parenchyma.

treatment planning and outcome. In the early stages of metastatic process, periportal and subcapsular locations are commonly affected (27). Perivenous areas may also be infiltrated in the course of metastatic liver disease and vascular invasion may be seen in select cases (Fig. 6).

Lymphoma

Lymphomatous involvement of the liver is a common clinical phenomenon and may be encountered in 50% of patients with non-Hodgkin lymphoma. Primary lymphoma of the liver, in contrast to the secondary involvement, is much more rare and accounts for less than 1% of all non-Hodgkin type lymphomas (28, 29).

Secondary lymphomatous involvement of the liver may manifest as discrete parenchymal focal lesions in 90% of the cases (30). On US images, lymphomatous nodules generally appear as homogeneously hypoechoic lesions which may sometimes mimic cysts. The absence of posterior acoustic enhancement is a useful imaging

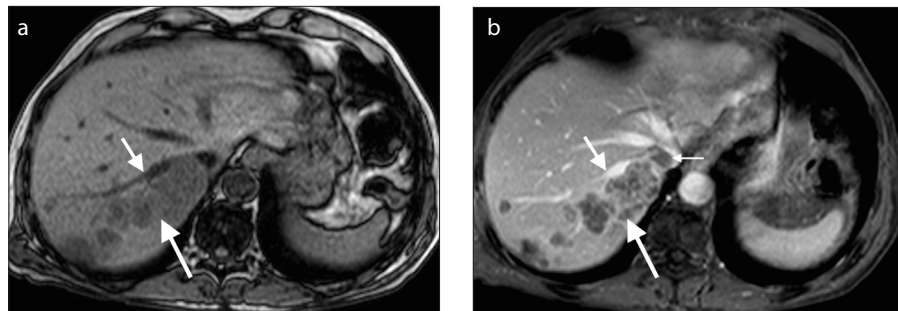


Figure 8. a, b. A 65-year-old woman with known hepatitis B presenting with increased alpha-fetoprotein level and general decline in her overall status. Axial T1-weighted unenhanced image (a) reveals multiple hypointense masses (long arrow) along the posterior border of right hepatic vein (short arrow). Axial contrast-enhanced T1-weighted image (b) at the venous phase demonstrates contrast wash-out in the lesions (long arrow) consistent with HCC. The tumor infiltrated the perivenous hepatic parenchyma (short arrow) and the hepatic vein with extension into the IVC (thin arrow).

clue in these patients by indicating the solid nature of these lesions. Nodules may sometimes have a bull's-eye appearance (30). CT is also a commonly utilized modality where these lymphomatous nodules generally appear as hypodense lesions, with attenuation values higher than that of water (30). On MRI, these nodules are typically hypointense compared with the background liver parenchyma on pre- and post-contrast T1-weighted images, with mild corresponding hyperintensity on T2-weighted images. Perivenous involvement may be also seen in these patients. The piercing vessel sign, which indicates a vessel branch traversing a focal lesion, without any associated luminal narrowing or occlusion, may be an important diagnostic clue. This sign is an indirect finding of the soft consistency of these lymphomatous deposits, which is in significant contrast with the hard consistency of the metastases from primary adenocarcinoma (Fig. 7).

Hepatocellular cancer

Hepatocellular cancer (HCC) is the most common primary liver tumor with potentially grave clinical prognosis. The invasion of major hepatic venous structures is an indicator of grave clinical prognosis in major HCC staging systems, with almost no chance of complete clinical cure reported in these patients (31). There is no universal consensus on the best treatment approach to patients with macroscopic hepatic venous invasion but both surgery and systemic chemotherapy have been proposed for best outcomes (32). Portal vein and its branches are the most commonly involved vessels within the liver, and hepatic venous invasion is much more rare compared with the portal vein invasion (33). As the hepatic veins finally drain

into the right atrium, potential pulmonary metastases would be expected to occur in these patients; however, it was reported that the most frequent site of recurrence in these patients was again the liver itself (32). CT and MRI are both very useful in diagnosing the hepatic vein invasion. Compared with bland thrombus, one should expect to see arterial phase enhancement within the thrombus, which basically points to the cellular nature of the tumor thrombus. The expansion of the involved hepatic vein is also a good indicator for tumor thrombus as neoplastic thrombi mostly do not respect the tissue and vessel wall boundaries (Fig. 8).

The evaluation of overall endovascular tumor load and outlining the degree of extension must be thoroughly evaluated, as these parameters have a significant potential in the selection of the optimal medical and surgical treatment approaches. Both CT and MRI may be successfully used to answer these critical questions.

Differentiation between neoplastic and non-neoplastic diseases in perivenous space

Non-neoplastic diseases involving the perivenous space perivenous space usually present with linear extension along the perivenous space. Neoplastic diseases involving the perivenous space can be differentiated from non-neoplastic diseases using the imaging features including mass effect on adjacent vascular and biliary structures, vascular invasion in hepatocellular carcinoma, contrast enhancement pattern on contrast-enhanced CT or MRI, diffusion restriction on diffusion-weighted imaging and perihepatic malignant lymph nodes if present (34, 35).

Conclusion

Perivenous space in the liver may be affected by various non-neoplastic and neoplastic conditions. Perivenous hypodensity/hypointensity is a common but nonspecific finding and may indicate edema due to various disease processes or fat infiltration. Several primary and secondary tumors may also invade perivenous space and awareness of the imaging clues may be of significant help to the imaging specialists not only in narrowing the differential diagnosis list but also in making confident diagnoses.

Conflict of interest disclosure

The authors declared no conflicts of interest.

References

1. Desser TS, Sze DY, Jeffrey RB. Imaging and intervention in the hepatic veins. *AJR Am J Roentgenol* 2003; 180:1583–1591. [\[CrossRef\]](#)
2. Lafortune M, Madore F, Patriquin H, Breton G. Segmental anatomy of the liver: a sonographic approach to the Couinaud nomenclature. *Radiology* 1991; 181:443–448. [\[CrossRef\]](#)
3. Cheng YF, Huang TL, Chen CL, et al. Variations of the middle and inferior right hepatic vein: application in hepatectomy. *J Clin Ultrasound* 1997; 25:175–182.
4. Fang CH, You JH, Lau WY, et al. Anatomical variations of hepatic veins: three-dimensional computed tomography scans of 200 subjects. *World J Surg* 2012; 36:120–124. [\[CrossRef\]](#)
5. Makuuchi M, Hasegawa H, Yamazaki S, Bandai Y, Watanabe G, Ito T. The inferior right hepatic vein: ultrasonic demonstration. *Radiology* 1983; 148:213–217. [\[CrossRef\]](#)
6. Sato TJ, Hirai I, Murakami G, Kanamura T, Hata F, Hirata K. An anatomical study of short hepatic veins, with special reference to delineation of the caudate lobe for hanging maneuver of the liver without the usual mobilization. *J Hepatobiliary Pancreat Surg* 2002; 9:55–60. [\[CrossRef\]](#)
7. Pupulim LF, Vilgrain V, Ronot M, Becker CD, Breguet R, Terraz S. Hepatic lymphatics: anatomy and related diseases. *Abdom Imaging* 2015; 40:1997–2011. [\[CrossRef\]](#)
8. Ohtani O, Ohtani Y. Lymph circulation in the liver. *Anat Rec (Hoboken)* 2008; 291:643–652. [\[CrossRef\]](#)
9. Marincek B, Barbier PA, Becker CD, Mettler D, Ruchti C. CT appearance of impaired lymphatic drainage in liver transplants. *AJR Am J Roentgenol* 1986; 147:519–523. [\[CrossRef\]](#)
10. Wells ML, Fenstad ER, Poterucha JT, et al. Imaging findings of congestive hepatopathy. *Radiographics* 2016; 36:1024–1037. [\[CrossRef\]](#)
11. Hamer OW, Aguirre DA, Casola G, Lavine JE, Woenckhaus M, Sirlin CB. Fatty liver: imaging patterns and pitfalls. *Radiographics* 2006; 26:1637–1653. [\[CrossRef\]](#)
12. Hamer OW, Aguirre DA, Casola G, Sirlin CB. Imaging features of perivascular fatty infiltration of the liver: initial observations. *Radiology* 2005; 237:159–169. [\[CrossRef\]](#)
13. Mahgerefteh SY, Sosna J, Bogot N, Shapira MY, Pappo O, Bloom AI. Radiologic imaging and intervention for gastrointestinal and hepatic complications of hematopoietic stem cell transplantation. *Radiology* 2011; 258:660–671. [\[CrossRef\]](#)
14. DeLeve LD, Shulman HM, McDonald GB. Toxic injury to hepatic sinusoids: sinusoidal obstruction syndrome (veno-occlusive disease). *Semin Liver Dis* 2002; 22:27–42. [\[CrossRef\]](#)
15. Torrisi JM, Schwartz LH, Gollub MJ, Ginsberg MS, Bosl GJ, Hricak H. CT findings of chemotherapy-induced toxicity: what radiologists need to know about the clinical and radiologic manifestations of chemotherapy toxicity. *Radiology* 2011; 258:41–56. [\[CrossRef\]](#)
16. Mehta NN, Ravikumar R, Coldham CA, et al. Effect of preoperative chemotherapy on liver resection for colorectal liver metastases. *Eur J Surg Oncol* 2008; 34:782–786. [\[CrossRef\]](#)
17. Nakano H, Oussoultzoglou E, Rosso E, et al. Sinusoidal injury increases morbidity after major hepatectomy in patients with colorectal liver metastases receiving preoperative chemotherapy. *Ann Surg* 2008; 247:118–124. [\[CrossRef\]](#)
18. Rubbia-Brandt L, Audard V, Sartoretto P, et al. Severe hepatic sinusoidal obstruction associated with oxaliplatin-based chemotherapy in patients with metastatic colorectal cancer. *Ann Oncol* 2004; 15:460–466. [\[CrossRef\]](#)
19. Shin NY, Kim MJ, Lim JS, et al. Accuracy of gadoxetic acid-enhanced magnetic resonance imaging for the diagnosis of sinusoidal obstruction syndrome in patients with chemotherapy-treated colorectal liver metastases. *Eur Radiol* 2012; 22:864–871. [\[CrossRef\]](#)
20. Ward J, Guthrie JA, Sheridan MB, et al. Sinusoidal obstructive syndrome diagnosed with superparamagnetic iron oxide-enhanced magnetic resonance imaging in patients with chemotherapy-treated colorectal liver metastases. *J Clin Oncol* 2008; 26:4304–4310. [\[CrossRef\]](#)
21. Elsayes KM, Shaaban AM, Rothan SM, et al. A comprehensive approach to hepatic vascular disease. *Radiographics* 2017; 37:813–836. [\[CrossRef\]](#)
22. Hommeyer SC, Teeffey SA, Jacobson AF, et al. Venocclusive disease of the liver: prospective study of US evaluation. *Radiology* 1992; 184:683–686. [\[CrossRef\]](#)
23. Erturk SM, Mortelet KJ, Binkert CA, et al. CT features of hepatic venoocclusive disease and hepatic graft-versus-host disease in patients after hematopoietic stem cell transplantation. *AJR Am J Roentgenol* 2006; 186:1497–1501. [\[CrossRef\]](#)
24. Koç Z, Uluhan S, Tokmak N. Hepatobiliary fascioliasis: imaging characteristics with a new finding. *Diagn Interv Radiol* 2009; 15:247–251.
25. Dusak A, Onur MR, Cicek M, Firat U, Ren T, Dogra VS. Radiological imaging features of fasciola hepatica infection - a pictorial review. *J Clin Imag Sci* 2012; 2:2. [\[CrossRef\]](#)
26. Sica GT, Ji H, Ros PR. CT and MR imaging of hepatic metastases. *AJR Am J Roentgenol* 2000; 174:691–698. [\[CrossRef\]](#)
27. Singh A, Chandrashekhara SH, Handa N, Balian V, Kumar P. “Periportal neoplasms”—a CT perspective: review article. *Br J Radiol* 2016; 89:20150756. [\[CrossRef\]](#)
28. Freeman C, Berg JW, Cutler SJ. Occurrence and prognosis of extranodal lymphomas. *Cancer* 1972; 29:252–260.
29. Tomasian A, Sandrasegaran K, Elsayes KM, Shanbhogue A, Shaaban A, Menias CO. Hematologic malignancies of the liver: spectrum of disease. *Radiographics* 2015; 35:71–86. [\[CrossRef\]](#)
30. Leite NP, Kased N, Hanna RF, et al. Cross-sectional imaging of extranodal involvement in abdominopelvic lymphoproliferative malignancies. *Radiographics* 2007; 27:1613–1634. [\[CrossRef\]](#)
31. Forner A, Llovet JM, Bruix J. Hepatocellular carcinoma. *Lancet* 2012; 379:1245–1255. [\[CrossRef\]](#)
32. Kokudo T, Hasegawa K, Yamamoto S, et al. Surgical treatment of hepatocellular carcinoma associated with hepatic vein tumor thrombosis. *J Hepatol* 2014; 61:583–588. [\[CrossRef\]](#)
33. Kokudo T, Hasegawa K, Matsuyama Y, et al. Liver resection for hepatocellular carcinoma associated with hepatic vein invasion: a Japanese nationwide survey. *Hepatology* 2017; 66:510–517. [\[CrossRef\]](#)
34. Seçil M, Obuz F, Altay C, et al. The role of dynamic subtraction MRI in detection of hepatocellular carcinoma. *Diagn Interv Radiol* 2008; 14:200–204.
35. Tarhan NC, Hatipoğlu T, Ercan E, et al. Correlation of dynamic multidetector CT findings with pathological grades of hepatocellular carcinoma. *Diagn Interv Radiol* 2011; 17:328–333.